Hyperscaling violation in the 2D 8-state Potts model with long-range correlated disorder

Christophe Chatelain

Hyperscaling violation in the 2D 8-state Potts model with long-range correlated disorder

C. Chatelain[1,2]

[1] *School of Physics, Indian Institute of Science Education and Research (IISER), Thiruvananthapuram, India*
[2] *Groupe de Physique Statistique, Département P2M, Institut Jean Lamour (CNRS UMR 7198), Université de Lorraine, France*

PACS 64.60.De – Statistical mechanics of phase transitions in model systems
PACS 05.50.+q – Potts models in lattice theory and statistics
PACS 05.70.Jk – Critical phenomena in thermodynamics
PACS 05.10.Ln – Monte Carlo methods in statistical physics and nonlinear dynamics

Abstract – The first-order phase transition of the two-dimensional eight-state Potts model is shown to be rounded when long-range correlated disorder is coupled to energy density. Critical exponents are estimated by means of large-scale Monte Carlo simulations. In contrast to uncorrelated disorder, a violation of the hyperscaling relation $\gamma/\nu = d - 2x_\sigma$ is observed. Even though the system is not frustrated, disorder fluctuations are strong enough to cause this violation in the very same way as in the 3D random-field Ising model. In the thermal sector too, evidence is given for such violation in the two hyperscaling relations $\alpha/\nu = d - 2x_\varepsilon$ and $1/\nu = d - x_\varepsilon$. In contrast to the random field Ising model, at least two hyperscaling violation exponents are needed. The scaling dimension of energy is conjectured to be $x_\varepsilon = a/2$, where a is the exponent of the algebraic decay of disorder correlations.

Introduction. – Quenched disorder when coupled to the energy density, say by dilution or random couplings, is known to soften first-order phase transitions. As argued by Imry and Wortis [1], local fluctuations of impurity concentration can destabilise the ordered phases in coexistence at the transition temperature if the surface tension is sufficiently small. In 2D, it was rigorously proved that an infinitesimal amount of disorder is sufficient to make any first-order transition continuous [2, 3]. The complete vanishing of the latent heat was first observed numerically in the case of the 2D 8-state Potts model [4]. The critical behaviour of the disorder-induced second-order phase transition is governed by a new random fixed point [5]. The universality class was later shown to depend on the number of states q [6]. In 3D, a finite disorder is required to round completely the first-order phase transition. The phase diagram exhibits a tricritical point separating a first-order regime from the disorder-induced continuous one, as first observed in the bond-diluted 4-state Potts model [7]. A rounding of the first-order phase transition of the 2D Potts model was also reported for anisotropic aperiodic sequences of couplings [8], and for layered random couplings [9, 10]. In both cases, the couplings are infinitely correlated in one direction. In the random case, the critical behaviour was shown to be governed by a q-independent infinite-randomness fixed point. The critical exponents are therefore those of the layered random Ising model, the celebrated McCoy-Wu model [11, 12]. Interestingly, the same critical behaviour is observed for the Potts model with homogeneous uncorrelated disorder in the limit $q \to +\infty$ [13].

In this letter, we consider the case of random bond couplings $J_{ij} > 0$ with algebraically decaying correlations $\overline{(J(0) - \bar{J})(J(\vec{r}) - \bar{J})} \sim r^{-a}$. According to the Imry-Wortis criterion, the low-temperature phase is destabilised when the fluctuations of exchange energy inside a ferromagnetic domain of characteristic length ℓ, increase faster with ℓ than the interface free energy $\sigma\ell^{d-1}$. Since the contribution of correlations to these fluctuations reads

$$\sqrt{\overline{\Big[\sum_{i,j}(J_{ij} - \bar{J})\Big]^2}} \sim \left[\ell^d \int_{\ell^d} \frac{d^d\vec{r}}{r^a}\right]^{1/2} \sim \ell^{d-a/2}, \quad (a \le d) \tag{1}$$

we expect the first-order phase transition to be softened for $a \le 2$ in the two-dimensional case. For $a > d$ and uncorrelated disorder, the main contribution is due to the

fluctuation term $\sqrt{\sum_{i,j}\overline{(J_{ij}-\bar{J})^2}} \sim \ell^{d/2}$. The case of an uncorrelated disorder is therefore equivalent to $a = d$. Unexpectedly, we observe that the critical exponents at the randomness-induced second-order phase transition do not satisfy hyperscaling relations. Such a violation had only been reported in random systems with frustration, spin glasses or random-field systems, but, to our knowledge, never for purely ferromagnetic systems. In the first section of this letter, the details of the Monte Carlo simulation are presented. Hyperscaling violation is studied first in the magnetic sector and then in the energy sector.

Description of the simulation. – We consider the 2D q-state Potts model with Hamiltonian

$$-\beta H = \sum_{(i,j)} J_{ij}\delta_{\sigma_i,\sigma_j} \tag{2}$$

where $\sigma_i \in \{0, 1, \ldots, q-1\}$ and the sum extends over pairs of nearest neighbours of the square lattice. We restrict ourselves to the case $q = 8$ for which the correlation length of the pure model is $\xi \simeq 24$ at the transition temperature. The order parameter m is defined as

$$m = \frac{q\rho_{\max} - 1}{q-1}, \quad \rho_{\max} = \max_\sigma \frac{1}{N}\sum_i \delta_{\sigma_i,\sigma} \tag{3}$$

where $\rho_{\max}$ is the density of spins in the majority state. This definition breaks the $\mathbb{Z}_q$ symmetry of the Hamiltonian in the same way as an infinitesimal magnetic field. In the case $q = 2$ corresponding to the Ising model, the usual order parameter $\frac{1}{N}\langle|\sum_i \sigma_i|\rangle$ is recovered.

We consider a binary distribution of coupling constants $J_{ij} \in \{J_1, J_2\}$ with

$$\left(e^{J_1} - 1\right)\left(e^{J_2} - 1\right) = q. \tag{4}$$

In the case of uncorrelated disorder, Eq. (4) is the self-duality condition that gives the location of the critical line. The ratio $r = J_2/J_1$ is used as a measure of the strength of disorder. Here, we present results for the case $r = 8$. To generate correlated coupling configurations $\{J_{ij}\}$, we simulate another spin model, namely the Ashkin-Teller model ($\sigma_i, \tau_i = \pm 1$)

$$-\beta H^{\mathrm{AT}} = \sum_{(i,j)} \left[J^{\mathrm{AT}}\sigma_i\sigma_j + J^{\mathrm{AT}}\tau_i\tau_j + K^{\mathrm{AT}}\sigma_i\sigma_j\tau_i\tau_j\right] \tag{5}$$

at different points of its critical line $e^{-2K^{\mathrm{AT}}} = \sinh 2J^{\mathrm{AT}}$. Two symmetries of the Hamiltonian are spontaneously broken at low temperatures: the global reversal of the spins σ_i and the reversal of both σ_i and τ_i. Therefore, two order parameters can be defined, magnetisation $\sum_i \sigma_i$ and polarisation $\sum_i \sigma_i\tau_i$, leading to two independent scaling dimensions:

$$\beta_\sigma^{\mathrm{AT}} = \frac{2-y}{24-16y}, \qquad \beta_{\sigma\tau}^{\mathrm{AT}} = \frac{1}{12-8y} \tag{6}$$

wherein we use the parametrization

$$\cos\frac{\pi y}{2} = \frac{1}{2}\left[e^{4K^{\mathrm{AT}}} - 1\right], \quad (y \in [0; 4/3]). \tag{7}$$

The correlation length exponent is $\nu^{\mathrm{AT}} = \frac{2-y}{3-2y}$. Spin configurations of this model are generated by Monte Carlo simulation using a cluster algorithm [14]. For each of them, a coupling configuration of the Potts model is constructed as

$$J_{ij} = \frac{J_1 + J_2}{2} + \frac{J_1 - J_2}{2}\sigma_i\tau_i, \tag{8}$$

where the site j is either at the right or below the site i. This construction ensures that the constraint (4) implies the self-duality of our random Potts model. Since the Askin-Teller is considered on its critical line, disorder fluctuations are self-similar and the coupling constants display algebraic correlations

$$\overline{(J_{ij} - \bar{J})(J_{kl} - \bar{J})} \sim |\vec{r}_i - \vec{r}_k|^{-a} \tag{9}$$

at large distances with

$$a = 2\beta_{\sigma\tau}^{\mathrm{AT}}/\nu^{\mathrm{AT}} = \frac{1}{4-2y}. \tag{10}$$

We have considered six points on the critical line, $y \in \{0, 0.25, 0.50, 0.75, 1, 1.25\}$, leading to six correlated disorder distributions with $a \simeq 0.25$, 0.286, 0.333, 0.4, 0.5 and 0.667. We have checked that disorder fluctuations display the expected scaling behaviour. The electric susceptibility of the Ashkin-Teller model, defined as

$$\chi^{\mathrm{AT}} = L^d\left[\overline{p^2} - \overline{|p|}^2\right] \tag{11}$$

where $p = \frac{1}{N}\sum_i \sigma_i\tau_i$ is the polarisation density, is computed. According to the fluctuation-dissipation theorem, this quantity is equal to the integral of the correlations (9) over the volume of the system. It is therefore expected to scale as L^{d-a}. The data are plotted on figure 1. A nice power-law behaviour is observed over the whole range of lattice sizes that are considered. The fitted exponents are given in Tab. 1 for all values of y. For $y \geq 0.75$, they are compatible with exact exponents. For smaller values of y, the deviation to the exact result is at most of 5%. Note that for $y = 0$, the Ashkin-Teller model is equivalent to the 4-state Potts model. The critical behaviour is therefore affected by logarithmic corrections. These values have been obtained with, and only with, the coupling configurations used during the simulation of the Potts model with correlated disorder. The agreement with the expected values, even for small lattice sizes, indicates that the number of disorder configurations is sufficient to reproduce correctly the expected disorder fluctuations.

For comparison, simulations for the Potts model with uncorrelated disorder are also performed. The same simulation code is used but with an infinite temperature of the

Table 1: Critical exponents $d-a$ of the electric susceptibility $\chi^{\rm AT}$ of the Ashkin-Teller model, or equivalently of fluctuations of the couplings J_{ij}, for different values of the parameter y. The numerical estimate of $d-a$ is denoted by MC (second line) and the exact value by Th. (third line).

y	0	0.25	0.5	0.75	1	1.25
$d-a$ (MC)	1.80(3)	1.80(3)	1.73(4)	1.61(3)	1.50(3)	1.34(2)
$d-a$ (Th.)	1.75	1.714	1.667	1.600	1.500	1.333

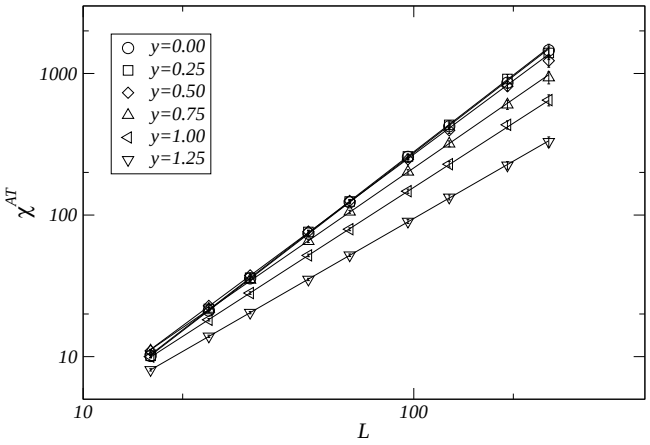

Fig. 1: Electric susceptibility $\chi^{\rm AT}$ of the Ashkin-Teller model, or equivalently fluctuations of the couplings J_{ij}, versus the lattice size L. The different symbols correspond to different values of the parameter y of the Ashkin-Teller model. The straight lines are power-law fits to the data.

Ashkin-Teller model in order to obtain uncorrelated spins and therefore uncorrelated couplings J_{ij}.

The Potts model is then simulated using the Swendsen-Wang algorithm [15]. Lattice sizes between $L = 16$ and 256 are considered. For each disorder configuration, 1000 MCs are performed to thermalise the system and $20,000$ MCs for data accumulation (auto-correlation time is $\tau \simeq 2$ for $L = 256$). Thermodynamic quantities are averaged over a number of disorder configurations proportional to $1/L^2$. For the largest lattice size $L = 256$, 2560 disorder configurations are generated while for $L = 64$ for instance, this number is raised up to 40960. Stability of disorder averages is checked. In the following, we will denote $\langle X\rangle$ the average of an observable over thermal fluctuations and $\overline{\langle X\rangle}$ the average of the latter over disorder.

On the critical line, the typical spin configurations of the Ashkin-Teller model display a large cluster of polarisation $\sigma\tau = +1$ or -1. As a consequence, our random coupling configurations also exhibit large clusters of either strong or weak bonds. The probability distribution of the total energy of the Potts model shows two peaks corresponding to these two kinds of bond configurations. This distribution is highly correlated to the probability distribution of polarisation of the Ashkin-Teller model. Since the latter undergoes a second-order phase transition, the two peaks come closer as the lattice size is increased. Note that in our model, macroscopic region of strong couplings are not rare: they have a probability 1/2. Moreover, they have a fractal dimension $1 < d_f < 2$ determined by the Ashkin-Teller model and, in the thermodynamic limit, only one such macroscopic region is expected to be present in the system. For this reason, the transition is not smeared but rounded [16].

Magnetic sector. – We estimate critical exponents by Finite-Size Scaling. The exponent β/ν can be extracted from magnetisation $\overline{\langle m\rangle}$ and its moments $\overline{\langle m^n\rangle}$ with $n = 2, 3, 4$. We observe nice power laws without any significant correction to scaling. Our estimates of $x_\sigma = \beta/\nu$ evolve with a and range from 0.061(5) ($y = 0$) to 0.108(4) ($y = 1.25$), to be compared with 0.150(2) for uncorrelated disorder (Tab. 2). We then consider the average magnetic susceptibility, numerically computed via the fluctuation-dissipation theorem

$$\bar{\chi} = L^d \overline{\langle m^2\rangle - \langle m\rangle^2}. \qquad (12)$$

The data display large corrections to scaling (see Fig. 2). A cross-over is observed around $L = 48$, not far from the correlation length $\xi = 24$ of the pure 8-state Potts model. In the region $L \geq 96$, power-law fits give stable estimates for γ/ν going from 1.70(7) ($y = 0.00$) to 1.62(4) ($y = 1.25$), to be compared with 1.69(4) for uncorrelated disorder. The hyperscaling relation $\gamma/\nu = d - 2\beta/\nu$ is therefore not satisfied (see values in Tab 2). We shall identify disorder fluctuations as the origin of this hyperscaling violation, like in the 3D Random-Field Ising Model (RFIM). Consider the following decomposition:

$$\bar{\chi} = L^d\big[\overline{\langle m^2\rangle} - \overline{\langle m\rangle}^2\big] - L^d\big[\overline{\langle m\rangle^2} - \overline{\langle m\rangle}^2\big]. \qquad (13)$$

As observed on Fig. 2, the difference of the two terms (13) leaves an average susceptibility which is smaller by a factor rougly equal to 3 in the case of uncorrelated disorder while it is two orders of magnitude smaller for correlated disorder. The first term, when computed separately, displays a power law behaviour with an exponent $(\gamma/\nu)^*$ incompatible with γ/ν but in agreement with the hyperscaling relation (Tab. 2). The second term of (13), the so-called disconnected susceptibility, involves the ratio

$$R_m = \frac{\overline{\langle m\rangle^2} - \overline{\langle m\rangle}^2}{\overline{\langle m\rangle}^2}, \qquad (14)$$

which is expected to behave as $R_m \sim R_m(\infty) + \mathcal{A}L^{-\phi}$, if magnetisation is not self-averaging [17]. We indeed ob-

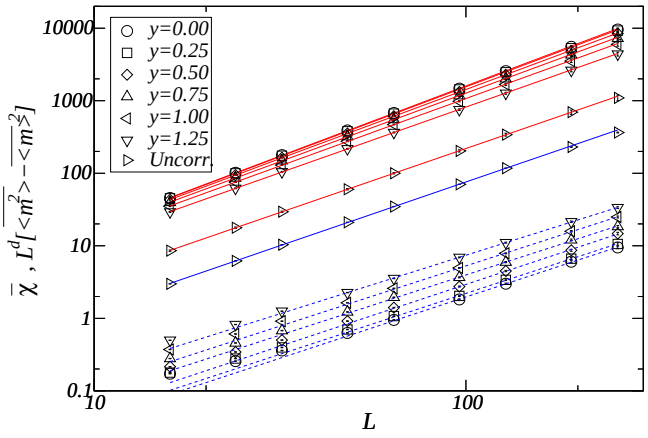

Fig. 2: Average magnetic susceptibility $\bar{\chi}$ (bottom) and $L^d[\overline{\langle m^2\rangle} - \overline{\langle m\rangle}^2]$ (top) versus lattice size L for different values of y and for uncorrelated disorder (Uncorr.). The straight lines correspond to power-law fits. Dashed lines indicate that the fit was performed over lattice sizes $L \geq 96$ only.

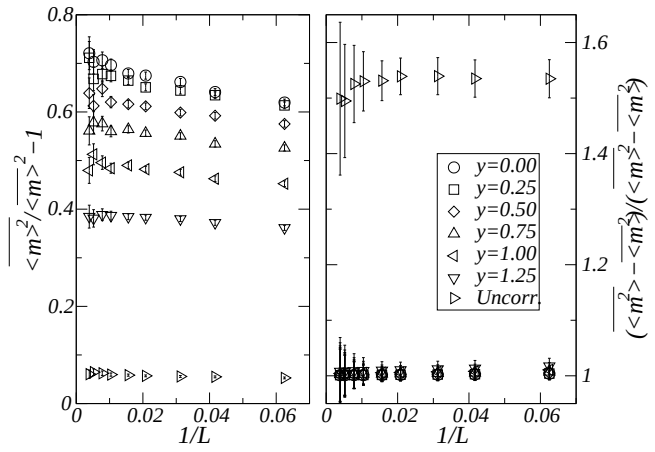

Fig. 3: On the left, ratio defined by Eq. (14) for different values of y and for uncorrelated disorder (Uncorr.) versus the inverse of the lattice size. The non-vanishing asymptotic limit, i.e. the extrapolated value on the y-axis, indicates that magnetization is not self-averaging for both correlated and uncorrelated disorder. On the right, ratio (15) of the two terms whose difference gives the average susceptibility. Asymptotically, this ratio displays a plateau at a value compatible with 1 for correlated disorder. For uncorrelated disorder, the asymptotic value is incompatible with 1.

serve that R_m goes to a non-vanishing constant in the limit $L \to +\infty$ (Fig. 3). The second term of Eq. (13) therefore behaves as $L^d\overline{\langle m\rangle}^2 \sim L^{d-2\beta/\nu}$, i.e. with an exponent satisfying the hyperscaling relation. Since the data indicate that it is also the case for the first term of Eq. (13), one can imagine that, if their amplitudes are equal, the dominant terms will cancel. To test this hypothesis, we compute the ratio

$$\frac{\overline{\langle m^2\rangle} - \overline{\langle m\rangle}^2}{\overline{\langle m\rangle^2} - \overline{\langle m\rangle}^2}. \tag{15}$$

We observe a plateau at 1.00(4) (Fig. 3). We therefore conclude that the hyperscaling violation is the result of an exact cancellation of the dominant contributions of the two terms of Eq. (13). The scaling of the average susceptibility is therefore determined by the first non-vanishing scaling correction $\bar{\chi} \sim L^{d-2\beta/\nu-\omega}$ of any of the two terms of Eq. (13) and the hyperscaling violation exponent θ is the exponent ω of this correction. Note that this is also the mechanism of hyperscaling violation invoked in the context of the RFIM [18] where our exponent $(\gamma/\nu)^*$ is denoted $4-\bar{\eta}$ [19,20]. In the case of uncorrelated disorder, the ratio (15) goes to a value significantly different from 1 in the large size limit (Fig. 3). The dominant contribution of the two terms of (13) do not cancel in this case and therefore hyperscaling is not violated.

Energy sector. – The divergence of specific heat is completely washed out by the introduction of disorder, which means that the specific heat exponent α/ν is either zero or negative (Fig 4). The average specific heat

$$\bar{C} = L^d\overline{< e^2 > - < e >^2} \tag{16}$$

can be decomposed in the same way as $\bar{\chi}$:

$$\bar{C} = L^d\left[\overline{\langle e^2\rangle} - \overline{\langle e\rangle}^2\right] - L^d\left[\overline{\langle e\rangle^2} - \overline{\langle e\rangle}^2\right]. \tag{17}$$

Like in the case of susceptibility, the two terms are several orders of magnitude larger than their difference for correlated disorder. We observe a nice power-law behaviour of the first term with an exponent in good agreement with $(\alpha/\nu)^* = (\gamma/\nu)^{\rm AT} = d - a$, which means that the fluctuations of energy are dominated by the fluctuations of the couplings and therefore of the polarisation density in the original Ashkin-Teller model. The second term involves the ratio R_e, constructed in the same way as R_m (14). Our numerical data show that energy is not self-averaging ($R_e(\infty) \neq 0$) and the ratio

$$\frac{\overline{< e^2 >} - \overline{< e >}^2}{\overline{< e >^2} - \overline{< e >}^2} \tag{18}$$

exhibits a plateau at the value 1.00(5) (Fig. 5). This implies the cancellation of the dominant contribution of the two terms of $\bar{C}$ so that a violation of the hyperscaling relation $\alpha/\nu = d - 2x_\varepsilon$ is expected. Even though we cannot measure x_ε from the scaling behaviour of energy, we infer that it can be extracted from the hyperscaling relation $(\alpha/\nu)^* = d - 2x_\varepsilon$ which implies $x_\varepsilon = a/2$. In the case of uncorrelated disorder, R_e is compatible with zero which means that energy is self-averaging and therefore the two dominant contributions of Eq. (17) do not cancel. As observed, hyperscaling is not violated in this case.

In pure systems, a good estimator for the determination of the correlation length exponent ν is

$$-\frac{d\ln\langle m\rangle}{d\beta} = L^d\frac{\langle me\rangle - \langle m\rangle\langle e\rangle}{\langle m\rangle}. \tag{19}$$

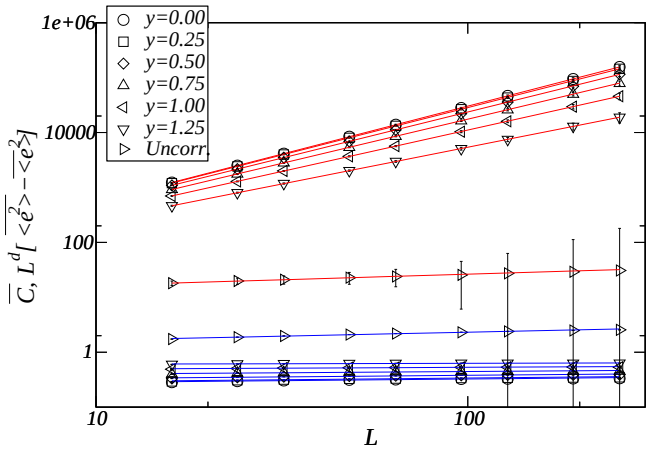

Fig. 4: Average specific heat $\bar{C}$ (bottom) and $L^d[\overline{\langle e^2\rangle} - \overline{\langle e\rangle}^2]$ (top) versus lattice size L for different values of y and uncorrelated disorder (Uncorr.). The straight lines correspond to power-law fits. For clarity, error bars of $\bar{C}$ in the uncorrelated case have been drawn as dashed line when they overlap with other points.

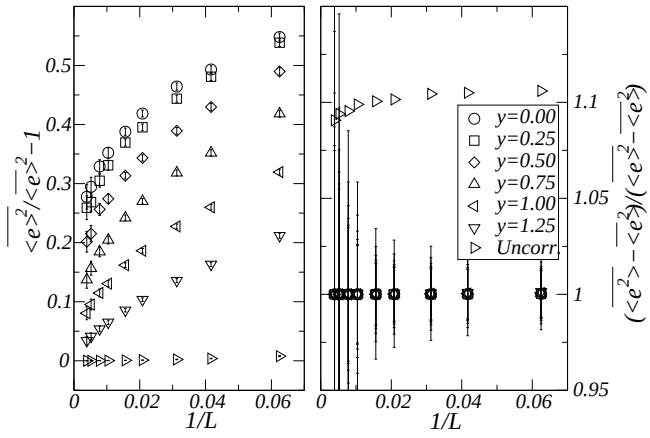

Fig. 5: On the left, ratio defined in the same way as Eq. (14), but for energy instead of magnetisation, versus the inverse of the lattice size L. A non-vanishing asymptotic limit is observed for correlated disorder, indicating that energy is not self-averaging in this case. On the right, ratio of the two terms whose difference gives the average specific heat. Error bars for uncorrelated disorder are large (they overlap other bars for large lattice sizes) and have not been represented for clarity. For correlated disorder, a plateau is observed at a value compatible with 1.

This is generalised to random systems as:

$$-\frac{d\ln\overline{\langle m\rangle}}{d\beta} = L^d \frac{\overline{\langle me\rangle} - \overline{\langle m\rangle\langle e\rangle}}{\overline{\langle m\rangle}}. \tag{20}$$

and is expected to scale as $d - x_\varepsilon$. A power-law fit to our data yields exponents $1/\nu$ close to zero but with large error bars. Consider again the decomposition

$$-\frac{d\ln\overline{\langle m\rangle}}{d\beta} = L^d \frac{\left[\overline{\langle me\rangle} - \overline{\langle m\rangle}\ \overline{\langle e\rangle}\right]}{\overline{\langle m\rangle}} - L^d \frac{\left[\overline{\langle m\rangle\langle e\rangle} - \overline{\langle m\rangle}\ \overline{\langle e\rangle}\right]}{\overline{\langle m\rangle}}. \tag{21}$$

The first term displays a power-law behaviour with exponents $1/\nu^*$ close to, though slightly above, $d - a/2$, which implies $x_\varepsilon \simeq a/2$ (Tab. 2). This estimate is consistent with the one obtained from the specific heat. The second term of (21) involves the ratio

$$R_{me} = \frac{\overline{\langle m\rangle\langle e\rangle} - \overline{\langle m\rangle}\ \overline{\langle e\rangle}}{\overline{\langle m\rangle}\ \overline{\langle e\rangle}}, \tag{22}$$

which behaves as $R_{me}(L) \sim R_{me}(\infty) + aL^{-\phi'}$ with $\phi' \simeq 0.3$. The constant $R_{me}(\infty)$ is clearly finite, except maybe for $y = 1.25$. Like in the magnetic case, the two terms of Eq. (21) have the same dominant scaling behaviour. The ratio

$$\frac{\overline{\langle me\rangle} - \overline{\langle m\rangle}\ \overline{\langle e\rangle}}{\overline{\langle m\rangle\langle e\rangle} - \overline{\langle m\rangle}\ \overline{\langle e\rangle}} \tag{23}$$

displays a plateau at 1.00(4) (Fig. 7). Consequently, the dominant contribution of the two terms of (21) is the same and they cancel. Hence, the hyperscaling relation $1/\nu = d - x_\varepsilon$ is expected to be violated. In the case of uncorrelated disorder, R_{me} is compatible with zero so we do not expect any cancellation of the two dominant contributions of Eq. (21) and, consequently, no hyperscaling violation.

Conclusions. – Numerical evidence has been given of the violation of hyperscaling relations in both the magnetic and energy sectors of the 2D 8-state Potts model with long-range correlated disorder. Even though this model is not frustrated, the mechanism causing these violations was shown to be the same as in the 3D RFIM, namely the cancellation of the two dominant contributions to the magnetic susceptibility, specific heat or derivative of the logarithm of magnetisation. However, there are two important differences between our Potts model with correlated disorder and the RFIM: disorder is coupled to the energy density and not magnetisation, and the random fixed point does not lie at zero temperature but at a finite temperature. The latter may explain why hyperscaling violation is observed in both magnetic and energy sectors. In the magnetic sector, the hyperscaling violation exponent is estimated to be $\theta_m = (\gamma/\nu)^* - \gamma/\nu \simeq 0.2$ while in the energy sector, $\theta_e = (\alpha/\nu)^* - \alpha/\nu \gtrsim d - a$ and $\theta'_e = (1/\nu)^* - 1/\nu \simeq d - a/2$. For uncorrelated RFIM, the hyperscaling violation exponent is compatible with $\theta \simeq d/2$. Since in the absence of correlation $a = d$, this value is identical to our estimate $\theta'_e = d - a/2$.

* * *

The author gratefully thanks Sreedhar Dutta and the Indian Institute for Science Education and Research (IISER) of Thiruvananthapuram for their warm hospitality and a stimulating environment.

Table 2: Critical exponents measured by Monte Carlo simulations (MC), or computed from them (from MC), and conjectured values (Conj.).

	y	0	0.25	0.5	0.75	1	1.25
	a	0.25	0.286	0.333	0.4	0.5	0.667
β/ν	(MC)	0.061(5)	0.060(5)	0.067(5)	0.075(5)	0.091(5)	0.108(4)
$d-2\beta/\nu$	(from MC)	1.88(1)	1.88(1)	1.87(1)	1.85(1)	1.82(1)	1.784(8)
γ/ν	(MC)	1.70(7)	1.69(8)	1.69(7)	1.67(8)	1.66(6)	1.62(5)
$(\gamma/\nu)^*$	(MC)	1.91(2)	1.90(3)	1.89(3)	1.87(3)	1.83(3)	1.79(3)
$(\alpha/\nu)^*$	(MC)	1.75(1)	1.73(2)	1.68(2)	1.61(2)	1.51(2)	1.34(2)
$d-a$	(conj.)	1.75	1.714	1.667	1.600	1.500	1.333
$1/\nu^*$	(MC)	1.90(2)	1.89(2)	1.86(2)	1.83(2)	1.78(2)	1.69(2)
$d-a/2$	(conj.)	1.875	1.857	1.835	1.8	1.75	1.667

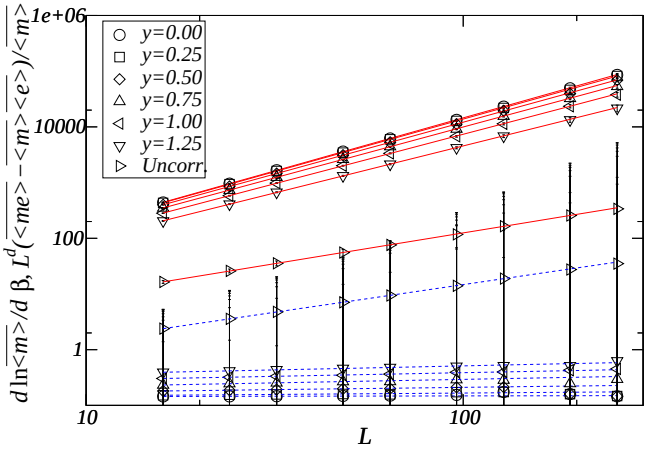

Fig. 6: Quantity $-\frac{d\ln\overline{\langle m\rangle}}{d\beta}$ (bottom) and $L^d\frac{\overline{\langle me\rangle}-\overline{\langle m\rangle}\,\overline{\langle e\rangle}}{\overline{\langle m\rangle}}$ (top) versus lattice size L for different values of y and for uncorrelated disorder (Uncorr.).

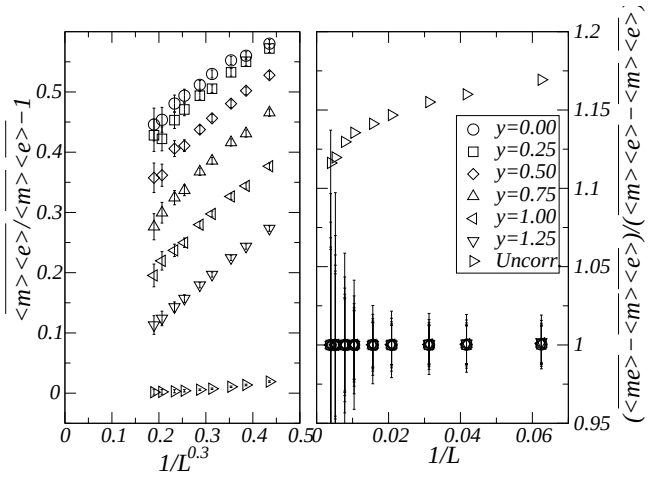

Fig. 7: On the left, ratio defined by Eq. (22) versus $1/L^{0.3}$. The non-vanishing extrapolation in the limit $L\to+\infty$ indicates that $\langle m\rangle$ and $\langle e\rangle$ are correlated in the case of correlated disorder. On the right, ratio (23) of the two terms whose difference gives $-\frac{d\ln\overline{\langle m\rangle}}{d\beta}$. Error bars for uncorrelated disorder are large and have not been represented for clarity. Again, a plateau compatible with 1 is observed for correlated disorder.

REFERENCES

[1] Imry Y. and Wortis M. *Phys. Rev. B* **19** 3580 (1979).

[2] Hui K. and Berker A.N. *Phys. Rev. Lett.* **62** 2507 (1989); Hui K. and Berker A.N. *Phys. Rev. Lett.* **63** 2433 (1989).

[3] Aizenman M. and Wehr J. *Phys. Rev. Lett.* **62** 2503 (1989); Aizenman M. and Wehr J. *Comm. Math. Phys.* **130** 489 (1990).

[4] Chen S., Ferrenberg A.M., and Landau D.P. *Phys. Rev. Lett.* **69** 1213 (1992); Chen S., Ferrenberg A.M., and Landau D.P. *Phys. Rev. E* **52** 1377 (1995).

[5] Chatelain C., and Berche B. *Phys. Rev. Lett.* **80** 1670 (1998).

[6] Olson T., and Young A.P. *Phys. Rev. B* **60** 3428 (1999), Chatelain C., and Berche B. *Phys. Rev. E* **60** 3853 (1999), Jacobsen J.L., and Picco M. *Phys. Rev. E* **61** R13 (2000).

[7] Chatelain C., Berche B., Janke W., and Berche P.-E. *Phys. Rev. E* **64** 036120 (2001).

[8] Berche P.-E., Chatelain C. and Berche B. *Phys. Rev. Lett.* **80** 297 (1998).

[9] Senthil T. and Majumdar S.N. *Phys. Rev. Lett.* **76** 3001 (1996).

[10] Carlon E., Chatelain C. and Berche B. *Phys. Rev. B* **60** 12974 (1999).

[11] McCoy B.M. and Wu T.T. *Phys. Rev.* **176** 631 (1968); McCoy B.M. and Wu T.T. *Phys. Rev.* **188** 982 (1969).

[12] Fisher D.S. *Phys. Rev. B* **51** 6411 (1995).

[13] Anglès d'Auriac J-Ch. and Iglói F. *Phys. Rev. Lett.* **90** 190601 (2003); Mercaldo M.T., Anglès d'Auriac J-Ch. and Iglói F. *Phys. Rev. E* **69** 056112 (2004).

[14] Salas J. and Sokal A.D. *J. Stat. Phys.* **85** 297 (1996).

[15] Swendsen R.H., and Wang J.S. *Phys. Rev. Lett.* **58** 86 (1987).

[16] Vojta T. *J. Phys. A.* **39** R143 (2006).

[17] Wiseman S., and Domany E. *Phys. Rev. E* **52** 3469 (1995).

[18] Schwartz M., and Soffer A. *Phys. Rev. Lett.* **55** 2499 (1985); Vojta T., and Schreiber M. *Phys. Rev. B* **52** R693 (1995)

[19] Bray A.J., and Moore M.A. *J. Phys. C* **18** L927 (1985).

[20] Fisher D.S. *Phys. Rev. Lett.* **56** 416 (1986).